

Agreement 58-1950-9-001 from the US Department of Agriculture, Agricultural Research Service; and the Research Training Program in Nutrition and Aging, Grant AG00209-09. We thank Dan Shaffer of Perkin-Elmer for help in designing the primers and probes.

#### References

1. Matarese V, Stone RL, Waggoner DW, Bernlohr DA. Intracellular fatty acid trafficking and the role of cytosolic lipid binding proteins. *Prog Lipid Res* 1989;28:245-72.
2. Baier LJ, Sacchetti JC, Knowler WC, Eads J, Paolisso G, Tataranni PA, et al. An amino acid substitution in the human intestinal fatty acid binding protein is associated with increased fatty acid binding, increased fat oxidation, and insulin resistance. *J Clin Invest* 1995;95:1281-7.
3. Hegele RA. A review of intestinal fatty acid binding protein gene variation and plasma lipoprotein response to dietary components [Review]. *Clin Biochem* 1998;31:609-12.
4. Baier LJ, Bogardus C, Sacchetti JC. A polymorphism in the human intestinal fatty acid binding protein alters fatty acid transport across Caco-2 cells. *J Biol Chem* 1996;271:10892-6.
5. Livak KJ, Marmaro J, Todd JA. Towards fully automated genome-wide polymorphism screening [Letter]. *Nat Genet* 1995;9:341-2.
6. Perkin-Elmer. TaqMan allelic discrimination protocol. Foster City, CA: Perkin-Elmer, 1998:1-3.

**High-Speed Apolipoprotein E Genotyping and Apolipoprotein B3500 Mutation Detection Using Real-Time Fluorescence PCR and Melting Curves, Charalampos Aslanidis\* and Gerd Schmitz** (Institute for Clinical Chemistry and Laboratory Medicine, University of Regensburg, Franz-Josef Strauss Allee 11, 93042 Regensburg, Germany; \* author for correspondence: fax 49 941 944 6202, e-mail Charalampos.Aslanidis@klinik.uni-regensburg.de)

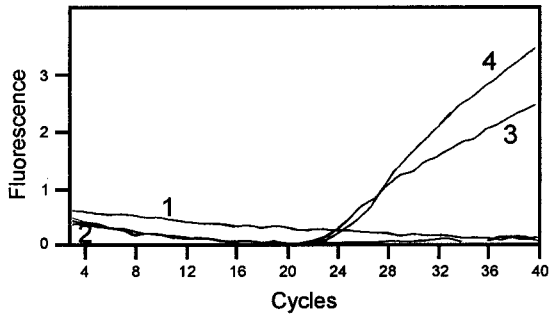
Apolipoproteins play a central role in cholesterol transport by their association to lipoproteins and their function as ligands for receptors, cofactors, or structural proteins. Mutations and polymorphisms in a variety of apolipoproteins lead to lipoprotein metabolism disorders and/or susceptibility to cardiovascular disease. In familial defective apolipoprotein B-100, the clearance of LDL particles from the circulation is impaired because of reduced affinity of the apolipoprotein (apo) B component of LDL for the LDL receptor as a result of a G-to-A mutation at nucleotide 10708 in exon 26 of the apoB gene, which causes substitution of Arg<sup>3500</sup> for Gln (1, 2). The frequency of the mutation is 1 in 700 in the general population (3). Heterozygous individuals have increased serum concentrations of cholesterol. Apolipoprotein E (apoE) likewise is involved in the clearance of HDL, contributing to reverse cholesterol transport (4). Genetic variation at the *APOE* locus in humans is an important determinant of plasma lipid concentrations and relative risk of atherosclerosis (5). Among several rare variants, three major alleles have been identified in the population: *E2*, *E3*, and *E4*. The most common *E3* isoform is distinguished by cysteine at position 112 and arginine at position 158 in the receptor-binding region of apoE. The *E4* isoform (Arg<sup>112</sup> and Arg<sup>158</sup>) is associated with increased cholesterol, thus enhancing the risk of heart disease (5). In addition, *E4/E4* individuals have a very high risk for developing Alzhei-

mer disease (6). Most patients with type III hyperlipidemia are homozygous for the *E2* allele (Cys<sup>112</sup> and Cys<sup>158</sup>).

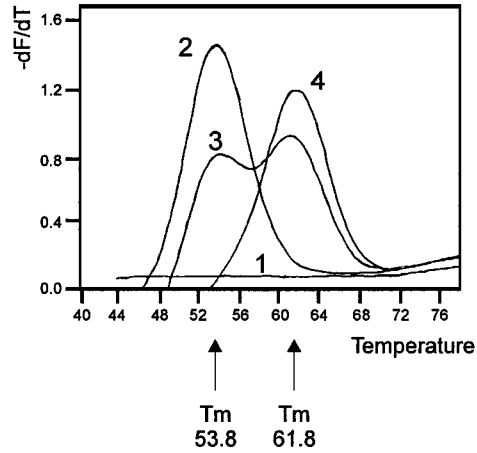
To date, genotyping for apoE is mainly performed by PCR, followed by digestion with restriction enzymes and restriction fragment length polymorphism (RFLP) analysis, and separation of the resulting DNA fragments on agarose or acrylamide gels (7). For apoB3500, an allele-specific PCR method is widely used (8). These nonhomogeneous methods give rise to unequivocal results, but they are time-consuming and require optimization of the PCR reaction to eliminate nonspecific PCR products, which would disturb the genetic analysis. Recently, a new detection methodology that relies on hybridization of amplicon-specific oligonucleotides with adjacent fluorophores capable of fluorescence resonance energy transfer has been introduced and used in a new high-speed thermal cycler (LightCycler; Roche Diagnostics) that uses glass capillaries and hot air for heating (9). This technology allows the real-time detection of the specific amplicon, followed by detection of the mutation by identification of the melting behavior of one of the two hybridization oligonucleotides (10). To this end, one hybridization primer matches the wild-type sequence (or mutant sequence), with the variable nucleotide in the middle of the sequence, and has LC-red640 as the fluorophore at its 5' end (detection probe, phosphorylated at 3' end); a second hybridization primer (anchor primer) is located proximally by a distance of one to three nucleotides and is labeled with fluorescein at its 3' end. During cycling, the hybridization probes hybridize the specific PCR product at the annealing temperature, and fluorescence is monitored. Cycling conditions are very fast because of temperature adjustments in the glass capillary (high surface-to-volume ratio). Following completion of the PCR, the PCR mixture is denatured and the temperature is lowered to 40 °C to facilitate binding of the hybridization probes, generating maximum fluorescence, and then slowly increased to 80 °C to permit melting of the detection probe, which is monitored by the decline of the fluorescence. This is being performed in the LightCycler itself, which has an integral device that enables denaturation and fluorescence detection. Melting curves are converted to melting peaks allowing easy distinction of the wild type from the mutant. The whole process is completed within 30 min.

We have used genomic DNA isolated from EDTA blood from individuals who previously had been typed by PCR-RFLP (apoE) and mutation-specific priming (apoB3500). The primers for the apoE PCR were CA1 5'-TTGAAGCCTCAAATCGGAAGT-3' and CA2 5'-CCGGCTGCCATCTCCTCCATCCG-3', which produce a 462-bp PCR product from genomic DNA. The primers for the apoB gene were UOL-A 5'-GGAGCAGTTGACCACAAGCTTAGCTTGG-3' and LOL-A 5'-AGAGTCCAGGGTGGCTTTGCTTGATG-3', which produced a 352-bp PCR product. The 3'-phosphorylated detection primer for apoE112 was E4-112M (LC-red640-ACATGGAGGACGTGCGCGG-p). The anchor primer E4-112A (CTGCAGGCGGCGCAGGCCCCGGCTGGCGC-fluorescein) was located proximal to the detection

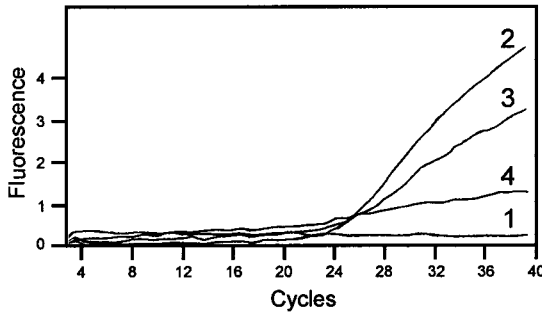
### apoE112



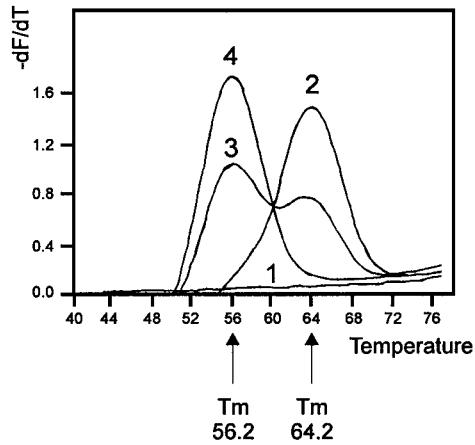
1 = H<sub>2</sub>O; 2 = E3/E3; 3 = E2/E4; 4 = E4/E4



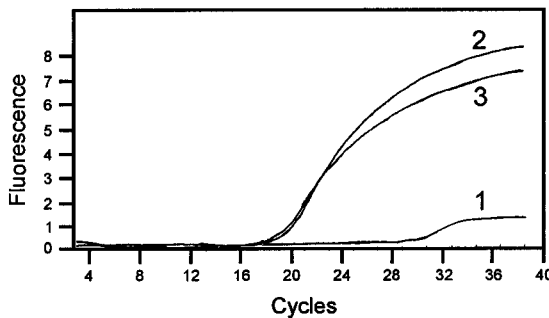
### apoE158



1 = H<sub>2</sub>O; 2 = E3/E3; 3 = E2/E4; 4 = E2/E2



### apoB3500



1 = H<sub>2</sub>O; 2 = apoB3500 heterozygous; 3 = wild type

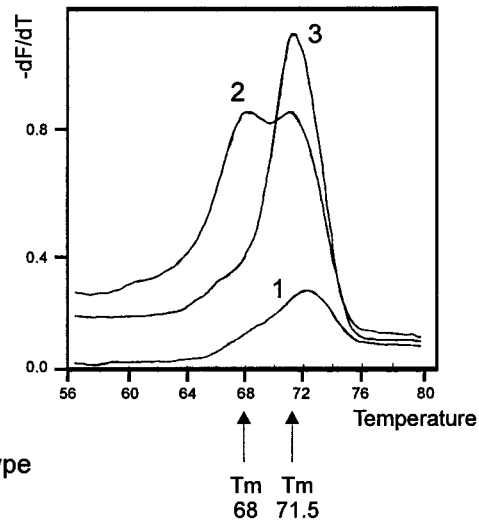


Fig. 1. Fluorescence vs cycle number (*left panels*) and melting peaks (*right panels*) for apoE genotyping and apoB3500 mutation detection.

DNAs from various individuals were amplified with apoE- or apoB-specific primers in glass capillaries (LightCycler), and fluorescence was monitored using apoE112-specific, apoE158-specific, and apoB3500-specific hybridization probes. The assignment of samples to curves is shown by numbers. Melting curves were converted to melting peaks by plotting the negative derivative of the fluorescence with respect to temperature ( $-dF/dT$ ) against temperature and are shown on the *right*. The melting point ( $T_m$ ) of the individual detection probes is shown by an *arrow*.

primer at a distance of two nucleotides. Likewise, the detection primer for apoE158 was E2-158M (LC-red640-GACCTGCAGAAGCGCCTGGC-p), and the anchor primer was E158A (GCTGCGTAAGCGGCTCCTCCGC-GATGCCG-fluorescein). Amplicon and mutation detection for apoB3500 was facilitated by the detection primer B3500M (red640-AGCTTCACTGAAGACCGTGTGCTCTTGGA-p) in combination with the anchor primer B3500A (GGTCCA-GATATCATCAATTTTGGAAAGTGCCCTG-fluorescein) at a distance of two nucleotides.

PCR and melting curve determination were performed in 20- $\mu$ L volumes in glass capillaries (Boehringer Mannheim). For apoE genotyping, the following pipetting scheme was used: 8.2  $\mu$ L of H<sub>2</sub>O, 1.8  $\mu$ L of 25 mmol/L MgCl<sub>2</sub>, 1  $\mu$ L each of 5 pmol/ $\mu$ L CA1 and CA2, 1  $\mu$ L each of E4-112A and E4-112M (for the apoE112 site) or E-158A and E2-158M (for the apoE158 site) from 4 pmol/ $\mu$ L stock solutions, 2  $\mu$ L of dimethyl sulfoxide, and 2  $\mu$ L of DNA-Master Hybridization Probes (Roche Diagnostics), containing Taq polymerase, reaction buffer, a dNTP mixture, and 10 mmol/L MgCl<sub>2</sub> as a 10 $\times$  concentrate. For apoB3500 mutation detection, 5.6  $\mu$ L of H<sub>2</sub>O, 2.4  $\mu$ L of 25 mmol/L MgCl<sub>2</sub>, 2  $\mu$ L each of 5 pmol/ $\mu$ L UOL-A and LOL-A, 2  $\mu$ L each of B3500M and B3500A from 4 pmol/ $\mu$ L stock solutions and 2  $\mu$ L of DNA-Master Hybridization Probes were added in a 20- $\mu$ L reaction. Genomic DNA (2  $\mu$ L, 50–200 ng) was used for amplification. Fluorescently labeled hybridization probes were synthesized by TIB MOLBIOL. Cycling conditions were identical for both applications, with initial denaturation at 94 °C for 2 min, followed by 40 cycles of denaturation 94 °C for 0 s, annealing at 60 °C for 10 s, and extension at 72 °C for 15 s, with a ramping rate of 20 °C/s. The fluorescence was monitored at the end of each 10-s annealing phase. After the products were amplified, we generated melting curves by denaturing the reaction at 95 °C for 0 s, holding the sample at 40 °C for 5 s, and then slowly heating the sample to 80 °C with a ramp rate of 0.2 °C/s, simultaneously monitoring the decline in fluorescence. We converted melting curves to melting peaks by plotting the negative derivative of the fluorescence with respect to temperature ( $-dF/dT$ ) against temperature.

The fluorescence profiles generated from selected DNA samples and negative controls are shown in Fig. 1. When the apoE112 hybridization probes were used (Fig. 1, top left), fluorescence increased constantly in the samples with the DNA (samples 3 and 4), whereas no fluorescence was detected in the control sample (H<sub>2</sub>O). Although no fluorescence was detectable in DNA sample 2, analysis of the PCR products on agarose gels revealed the presence of the specific PCR product. Sample 2 does not produce fluorescence because the detection hybridization probe for apoE112 is derived from the E4 allele, which leads to a mismatch in the PCR products (E3/E3), generating a low melting point (53.8 °C). The PCR cycling, however, has been performed at an annealing temperature of 60 °C. A reduction in the annealing temperature increases fluorescence during PCR cycling when DNA from an E3/E3 individual is used (data not shown). The melting curves

of the same samples are shown in Fig. 1 (top right). The melting point ( $T_m$ ) of the E3/E3 DNA (curve 2) was 53.8 °C, demonstrating the presence of specific PCR product in the reaction. The  $T_m$  of the E4/E4 DNA (curve 4) was 61.8 °C because the detection probe matches perfectly. The E2/E4 DNA (curve 3) showed melting peaks at 53.8 and 61.8 °C, demonstrating heterozygosity at position E112.

The fluorescence monitored with the hybridization probes specific for the apoE158 position is shown in Fig. 1 (middle left). The three DNA samples of different genotypes produced different fluorescence signals, although analysis of the PCR products on agarose gels revealed equal amounts of PCR product (data not shown). The detection probe of the apoE158 site was derived from the E4 allele and matched the sequence of the E4 and E3 alleles perfectly, leading to stable hybridization at the annealing temperature, whereas base pairing with PCR products from E2/E2 individuals was impaired because of a lower  $T_m$  (56.2 °C). This apparent variability in signal intensity did not affect the quality of the melting curves because monitoring of the melting behavior started at 40 °C, the temperature at which mismatched detection probes contribute equally to signal generation. The  $T_m$  of the E2/E2 sample (curve 4) was 56.2 °C, whereas the perfect match with the E3/E3 sample produced a  $T_m$  of 64.2 °C (curve 2). The sample of the heterozygous individual (curve 3) showed a two-phase melting behavior.

The detection probes used for apoE genotyping in the LightCycler revealed 8 °C differences in melting temperatures. A summary of the melting peaks of individual apoE genotypes is given in Table 1. The combination of the digits 1 and 0, with 1 meaning that the particular peak is present and 0 reflecting the absence, is unique and unambiguously determines the apoE genotype. The four individual  $T_m$ s (53.8, 56.2, 61.8, and 64.2 °C) are well separated. Using all hybridization probes simultaneously in one PCR reaction, we were able to identify individual melting peaks in some samples, but reliable genotyping was not possible (data not shown). Therefore, two separate PCR reactions with the respective hybridization probes are recommended for apoE genotyping. To date, we have analyzed >100 individuals with various apoE genotypes with the LightCycler and compared the data with the results obtained with traditional PCR-RFLP. The

**Table 1. apoE genotyping with melting peaks.**

Genotype	E112 probes		E158 probes	
	$T_m$ 53.8 °C	$T_m$ 61.8 °C	$T_m$ 56.2 °C	$T_m$ 64.2 °C
E2/E2	1	0	1	0
E3/E3	1	0	0	1
E4/E4	0	1	0	1
E2/E3	1	0	1	1
E2/E4	1	1	1	1
E3/E4	1	1	0	1

<sup>a</sup> 1, melting peak present; 0, melting peak absent.

genotypes were identical. The positions and distances of melting peaks were identical in individuals with the same genotypes.

The detection probe of the apoB3500 mutation was derived from the nonsense DNA strand and matched the wild-type sequence of the gene. Because of the length and base composition of the probe, the melting points were higher compared with the apoE probes. Therefore, the fluorescence signal intensity during PCR reaction was equally high for the DNA sample with the wild-type sequence (curve 3 in Fig. 1, bottom left) and the heterozygous individual (curve 2). The melting peaks were clearly differentiated ( $T_m$  68 and 71.5 °C). The rather similar melting behavior (compared with apoE) is attributable to the length and base composition of the probes. Using the same procedure as for apoE genotyping, we performed apoB3500 mutation analysis on different wild-type samples (different individuals and different DNA preparations) and samples from a heterozygous individual. The results were identical to the results obtained with gel-based technologies. There was no run-to-run variation of the melting points.

Compared with traditional PCR genotyping and mutation detection, applications can be adapted very easily on the LightCycler. We have established additional mutation detection protocols for methylenetetrahydrofolate reductase and prothrombin (manuscript in preparation). In our experience, the basis for the design of the PCR primers is the same as required for traditional thermal cyclers and protocols. Extensive optimization is not required; in fact, for apoB3500, methylenetetrahydrofolate reductase, and prothrombin, the PCR primers and cycle conditions did not need to be optimized at all. Because the DNA sequence of the apoE gene is GC-rich, PCR conditions and primers had to be optimized. Because of the nature of the generation of the fluorescence signal, contaminating, non-specific PCR products do not affect the results. The PCR primers for apoE described in this study generated a specific amplicon. With respect to the hybridization probes, a distance of two nucleotides between the anchor primer and the detection primer was ideal for efficient energy transfer and signal generation. The anchor primer (28–30 nucleotides in length) should enable hybridization at higher temperatures compared with the detection primer (~20 nucleotides in length). The mutant nucleotide should be positioned close to the middle of the detection primer. It is also important that the annealing temperature in the PCR reaction is kept below the melting point of the detection primer to allow monitoring of the fluorescence during the cycling.

In our opinion, the LightCycler technology is more accurate than traditional, gel-based assays because it enables the identification of the specific amplicon and uses this amplicon for mutation detection. It is conceivable that in a traditional method that uses PCR-RFLP, contaminating PCR products would scramble the analysis. In an allele-specific amplification (as performed for apoB3500), the quality of the discriminating primers is crucial.

We have established high-speed (30 min) and easy-to-perform genotyping for the apoE alleles and the identification of the apoB3500 mutation, using the LightCycler technology and melting curves. This homogeneous system minimizes PCR contamination concerns related to sample handling and does not require digestion of PCR products with restriction enzymes and/or fragment separation on gels.

#### References

1. Innerarity TL, Weisgraber KH, Arnold KS, Mahley RW, Kraus RM, Vega GL, et al. Familial defective apolipoprotein B-100: low density lipoproteins with abnormal receptor binding. *Proc Natl Acad Sci U S A* 1987;84:6919–23.
2. Soria LF, Ludwig EH, Clarke HR, Vega GL, Grundy SM, McCarthy BJ. Association between a specific apolipoprotein B mutation and familial defective apolipoprotein B-100. *Proc Natl Acad Sci U S A* 1989;86:587–91.
3. Schuster H, Rauh G, Kormann B, Hepp T, Humphries S, Keller C, et al. Familial defective apolipoprotein B-100. Comparison with familial hypercholesterolemia in 18 cases detected in Munich. *Arteriosclerosis* 1990;10:577–81.
4. Mahley RW. Apolipoprotein E: cholesterol transport protein with expanding role in cell biology. *Science* 1988;240:622–30.
5. Davignon J, Gregg RE, Sing CF. Apolipoprotein E polymorphism and atherosclerosis. *Arteriosclerosis* 1988;8:1–21.
6. Corder EH, Saunders AM, Strittmatter WJ, Schmechel DE, Gaskell PC, Small GW, et al. Gene dose of apolipoprotein E type 4 allele and the risk of Alzheimer's disease in late onset families. *Science* 1993;261:928–9.
7. Hixson JE, Vernier DT. Restriction isotyping of human apolipoprotein E by gene amplification and cleavage with *HhaI*. *J Lipid Res* 1990;31:545–8.
8. Schuster H, Rauh G, Müller S, Keller C, Wolfram G, Zöllner N. Allele-specific and asymmetric polymerase chain reaction amplification: a one step polymerase chain reaction protocol for rapid diagnosis of familial defective apolipoprotein B-100. *Anal Biochem* 1992;204:22–5.
9. Wittwer C, Ririe K, Andrew R, David D, Gundry R, Balis U. The LightCycler: a microvolume multisample fluorometer with rapid temperature control. *Bio-techniques* 1997;22:176–81.
10. Lay M, Wittwer C. Real-time fluorescence genotyping of factor V Leiden during rapid cycle PCR. *Clin Chem* 1997;43:2262–7.

---

**Biological Day-to-Day Variation and Reference Change Limits of Serum Cortisol and Aldosterone in Healthy Young Men on Unrestricted Diets, Outi Ahokoski,<sup>1,2\*</sup> Arja Virtanen,<sup>1</sup> Veli Kairisto,<sup>1</sup> Harry Scheinin,<sup>2</sup> Risto Huupponen,<sup>2</sup> and Kerttu Irjala<sup>1</sup>** (<sup>1</sup> Central Laboratory, Turku University Central Hospital, FIN-20520 Turku, Finland, and <sup>2</sup> Department of Pharmacology and Clinical Pharmacology, University of Turku, FIN-20520 Turku, Finland; \* author for correspondence: fax 358-2-2613920, e-mail outi.ahokoski@utu.fi)

Several factors are known to influence neuroendocrine secretion. A circadian rhythm with a clear episodic secretion of serum cortisol and aldosterone has been well described in several reports (1, 2). Recently, a gender-related seasonal periodicity in plasma cortisol was reported (3). However, in many of the studies on biological variability, the experimental setting has not reflected the routine daily living habits of the subjects. In the interpretation of laboratory results, especially in monitoring outpatients, the variability present in the routine environment should be taken into account.

Data on biological variation are needed for the correct interpretation of serial laboratory results in clinical prac-